

## Two Luminous Post-AGB Stars in the Galactic Globular Cluster M19

HOWARD E. BOND,<sup>1,2,3</sup> BRIAN D. DAVIS,<sup>1</sup> MICHAEL H. SIEGEL,<sup>1</sup> AND ROBIN CIARDULLO<sup>1,4</sup>

<sup>1</sup>*Department of Astronomy & Astrophysics, Pennsylvania State University, University Park, PA 16802, USA*

<sup>2</sup>*Space Telescope Science Institute, 3700 San Martin Drive, Baltimore, MD 21218, USA*

<sup>3</sup>*Visiting Astronomer, Cerro Tololo Inter-American Observatory, National Optical Astronomy Observatory, operated by the Association of Universities for Research in Astronomy under a cooperative agreement with the National Science Foundation.*

<sup>4</sup>*Institute for Gravitation and the Cosmos, Pennsylvania State University, University Park, PA 16802, USA*

Submitted to AJ

### ABSTRACT

We report the discovery of a luminous “yellow” post-asymptotic-giant-branch (PAGB) star in the globular cluster (GC) M19 (NGC 6273), identified during our *uBVI* survey of Galactic GCs. The *uBVI* photometric system is optimized to detect stars with large Balmer discontinuities, indicating very low surface gravities and high luminosities. The spectral-energy distribution (SED) of the star is consistent with an effective temperature of about 6250 K and a surface gravity of  $\log g = 0.5$ . We use *Gaia* data to show that the star’s proper motion and radial velocity are consistent with cluster membership. One aim of our program is to test yellow PAGB stars as candidate Population II standard candles for determining extragalactic distances. We derive a visual absolute magnitude of  $M_V = -3.39 \pm 0.09$  for the M19 star. This is in close agreement with the  $M_V$  values found for yellow PAGB stars in the GCs  $\omega$  Cen, NGC 5986, and M79, indicating a very narrow luminosity function. These objects are four magnitudes brighter than RR Lyrae variables, and they can largely avoid the issues of interstellar extinction that are a problem for Population I distance indicators. We also identified a second luminous PAGB object in M19, this one a hotter “UV-bright” star. Its SED is consistent with an effective temperature of about 11,750 K and  $\log g = 2.0$ . The two objects have nearly identical bolometric luminosities,  $\log L/L_\odot = 3.24$  and 3.22, respectively.

*Keywords:* stars: AGB and post-AGB — globular clusters: individual (M19) — distance scale — stars: evolution

### 1. YELLOW POST-AGB STARS IN GLOBULAR CLUSTERS

The visually brightest objects in globular clusters (GCs) and old stellar populations are stars in their final evolution from the tip of the asymptotic giant branch (AGB) toward higher temperatures in the color-magnitude diagram (CMD). As these post-AGB (PAGB) stars pass at nearly constant bolometric luminosity through spectral types early G, F, and late A, they reach their brightest visual absolute magnitudes, because of the dependence of the bolometric correction upon effective temperature.

It has been suggested (Bond 1997a,b) that these luminous “yellow” PAGB stars may be useful Population II standard candles. In populations containing only old stars there should be fairly sharp upper and lower limits to their brightnesses. In addition, yellow PAGB stars have conspicuously large Balmer discontinuities in their spectral-energy distributions (SEDs), making them easy to recognize using a single set of suitable photometric observations. They should be detectable in early-type galaxies that do not contain Cepheids, and in the halos of spirals, where there are fewer issues of interstellar extinction than there are for Population I distance indicators.

Because of the rapid evolutionary timescales for PAGB stars, however, these objects are very rare. The previously known luminous yellow PAGB stars in the Galactic GC system number only five: (1) HD 116745

(“Fehrenbach’s star,” ROA 24; [Gonzalez & Wallerstein 1992](#) and references therein) and the RV Tauri variable V1 in  $\omega$  Centauri ([Jones 1968](#)); (2) two luminous yellow PAGB stars in NGC 5986 ([Bond 1977](#); [Alves et al. 2001](#)); and (3) a yellow PAGB star in M79, discovered by [Bond et al. \(2016, hereafter B16\)](#). There are very few, if any, yellow stars in the CMDs of Galactic GCs that lie above the horizontal branch (HB) and within  $\sim 1$  magnitude of the brightness of these objects (see [Davis et al. 2021, hereafter D21](#)). Analogs of the GC objects are also known in the field; an example is the Galactic halo star BD+14°3061, along with a few other similar field objects ([Bond 2020, hereafter B20](#), and references therein).

In this paper, we report our discovery of a luminous yellow PAGB star in the Galactic GC M19 (NGC 6273). As described in detail in D21, this object was the only new luminous yellow PAGB star found in our photometric survey of nearly the entire known sample of Galactic GCs. Thus, it is likely to be the final member of this class in the Galactic GCs.

As PAGB stars continue to evolve, they reach high effective temperatures, and arrive at the top of the white-dwarf cooling sequence in the CMD. These hot, luminous objects are conspicuous at short wavelengths, especially in the ground- and space-based ultraviolet (UV). There is a substantial literature on these prominent, but rare, “UV-bright” objects in GCs, beginning with [Zinn et al. \(1972, hereafter ZNG\)](#), and summarized recently by [Moehler et al. \(2019\)](#), who list about three dozen known or candidate members of the class. Our observations of M19 also revealed a previously unrecognized luminous UV-bright PAGB star, and we briefly discuss this object as well.

## 2. OBSERVATIONS

In the mid-1990s, H.E.B. and collaborators began to develop a ground-based photometric system optimized for efficient discovery of luminous, low-gravity A, F, and G-type stars having large Balmer jumps. This “*uBVI*” system combines the [Thuan & Gunn \(1976\)](#) *u* filter, whose bandpass lies almost entirely shortward of the Balmer discontinuity,<sup>1</sup> with the broad-band *BVI* filters of the standard Johnson-Kron-Cousins system. The astrophysical motivations and design principles of the *uBVI* system were presented by [Bond \(2005, hereafter Paper I\)](#). [Siegel & Bond \(2005, hereafter Paper II\)](#) established a network of equatorial *uBVI* standard stars,

based on extensive CCD observations with 0.9-, 1.5-, and 4-m telescopes at Kitt Peak National Observatory (KPNO) and Cerro Tololo Inter-American Observatory (CTIO).

Over the years 1994 to 2001, H.E.B. made *uBVI* observations at KPNO and CTIO of nearly the entire known sample of Galactic GCs. The primary aim of this survey was to search systematically for yellow PAGB stars, with a goal of testing their potential as standard candles and to establish a photometric zero-point. A forthcoming paper (D21) will present a complete census of stars in the Galactic GC system lying above the HB, bluer than the red-giant branch and AGB, and redder than  $(B - V)_0 = -0.1$  in the cluster CMDs. Further papers will describe the zero-point calibration for yellow PAGB stars, and the results of searches for them in Local Group galaxies. This paper focuses on the luminous yellow PAGB star that the survey revealed in M19, as well as a luminous hot UV-bright member of the cluster.

*uBVI* survey observations of M19 were made with the CTIO 0.9-m telescope on 1998 April 21 ( $2 \times 2$  grid centered on the cluster; exposure times at each pointing were  $2 \times 800, 75, 40$ , and  $45$  s, respectively) and April 22 (cluster center; exposure times  $400, 75, 40$ , and  $45$  s). The field of view of the 0.9-m CCD camera was  $13' \times 13'$ . Exposure times in the *uBVI* filters on the second night were chosen so as to reach a signal-to-noise ratio of about 200–300 for stars about 2 mag brighter than the HB, allowing for interstellar extinction. The first night was not photometric, and the exposure times in *u* were lengthened.

M19 is a populous GC, one of the 10 or so most massive clusters in the Galactic GC system. [Kruijssen et al. \(2020\)](#), [Pfeffer et al. \(2020\)](#), and others have argued that it is the remnant nuclear star cluster of a dwarf galaxy (“Kraken”), which was disrupted and accreted by the Milky Way. M19 lies in the Galactic bulge in Ophiuchus ( $l = 356^\circ.9, b = +9^\circ.4$ ), and is overlain by a considerable number of field stars. Early work (e.g., [Harris et al. 1976](#)) showed that M19 is affected by substantial differential reddening, and that it has a very blue HB, consistent with low metallicity. The [Harris \(2010, hereafter H10\)](#) catalog of GC parameters<sup>2</sup> gives a metal content of  $[\text{Fe}/\text{H}] = -1.74$ . A recent spectroscopic study ([Johnson et al. 2017](#)) of over 300 red giants and AGB stars in the cluster showed that there is a range of iron contents among the members, from about  $[\text{Fe}/\text{H}] = -2$  to  $-1$ , but concentrated around  $-1.75$  and  $-1.5$ . These

<sup>1</sup> The Thuan-Gunn *u* bandpass is distinct from, and shortward of, that of the *u'* filter of the Sloan Digital Sky Survey, which partially overlaps the Balmer jump.

<sup>2</sup> Online version of 2010 December, at <http://physwww.mcmaster.ca/~harris/mwgc.dat>

findings are indicative of considerable self-enrichment in this massive GC.

### 3. DATA ANALYSIS AND SELECTION OF PAGB CANDIDATES

The CCD frames were reduced as described in detail by B16 and D21, using standard tasks in IRAF<sup>3</sup> for bias subtraction and flat-fielding. Instrumental stellar magnitudes were measured on the frames with the ALLSTAR and DAOGROW tasks in DAOPHOT (Stetson 1987). These data were corrected for atmospheric extinction, and then the 1998 April 22 frames were calibrated to the *uBVI* system using measurements of standard fields obtained during this observing run. We used the *u* magnitudes of standard stars from Paper II, and *BVI* magnitudes for the standards of Landolt (1992). Since the 1998 April 21 night was not photometric, its zero-points were determined by scaling to the M19 frames obtained on the photometric night. Finally, all of the measurements were combined into a single catalog of mean calibrated magnitudes. For the bright PAGB candidates considered here, the photometry provides essentially complete stellar samples into the cluster center (apart from rare cases of badly blended bright stars; see D21 for further discussion of the sample completeness for our GC survey).

We then searched for candidate yellow PAGB stars by choosing objects that are simultaneously bright, have large Balmer jumps, and have spatial locations and proper motions consistent with cluster membership. Figure 1 illustrates the selection process. The top two frames show two CMDs for the cluster, after correcting for a nominal cluster-averaged interstellar extinction of  $E(B - V) = 0.38$  (from H10), and assuming  $R_V = 3.1$ . (For the extinction corrections in  $V - I$ , we used the formula of Dean et al. 1978.) The top left panel plots  $V_0$  vs.  $(B - V)_0$ , and the top right plots  $V_0$  vs.  $(V - I)_0$ .

As noted in §2, M19 lies in the Galactic bulge, and there are substantial numbers of field stars in our CCD frames. To remove most of them from our *uBVI* catalog, we applied three constraints, based on spatial location and on astrometry of the stars given in the *Gaia* Data Release 2 (DR2; Gaia Collaboration et al. 2016, 2018)<sup>4</sup>: (1) angular distance from the cluster center less than three times the half-light radius (i.e.,  $3 \times 79''2$ , using the half-light radius given by H10); (2) DR2 proper motions

in right ascension and declination within  $1.1 \text{ mas yr}^{-1}$  of the cluster mean of  $(\mu_\alpha, \mu_\delta) = (-3.22, +1.61) \text{ mas yr}^{-1}$  (Gaia Collaboration et al. 2018); and (3) DR2 parallax less than 0.7 mas (to exclude objects almost certainly in the foreground). The top panels in Figure 1 show that these criteria result in a nearly pure sample of cluster members, especially brighter than  $V_0 \simeq 14$ ; but there do appear to be a few remaining field stars below that level.

Also shown in the top left panel is the approximate location of the RR Lyrae, Cepheid, and RV Tauri instability strip (e.g., Harris et al. 1983; D21). M19 contains seven objects listed in the Clement et al. (2001) catalog<sup>5</sup> of variable stars in GCs. However, two of them (V6 and V7) appear to be non-members, based on their proper motions in *Gaia* DR2. The positions of the remaining five variables in the CMDs in Figure 1, based on our photometry, are plotted as filled green circles. They consist of four Type II Cepheids<sup>6</sup> and one RR Lyrae variable. Our data are comprised of only a few measurements on two successive nights, made at random pulsation phases, so they should not be regarded as representing the time-averaged locations of the variables in the CMDs. Nevertheless, the RR Lyr variable, and three of the Cepheids, do lie inside, or on the border of, the schematic instability strip.

The red-giant branch (RGB) and HB of the cluster's CMD in Figure 1 have appreciable width (compare with, for example, the very narrow RGB and HB of the nearly unreddened GC M79 in our team's data, shown in Figure 1 of B16). This spread is partially due to substantial differential interstellar reddening across the face of M19—as we noted above, and has been discussed in several more recent studies of the cluster, including Piotto et al. (1999), Alonso-García et al. (2012), Johnson et al. (2017), and references therein to earlier literature.

As our index of the strength of the Balmer discontinuity, we use the color difference  $(u - B) - (B - V)$ , which is a broad-band analog of the  $c_1$  Balmer-jump index of the Strömgren *uvby* system.<sup>7</sup> In the bottom panel of Figure 1, we plot this color difference vs. the  $(V - I)_0$  temperature index, for the M19 members in the top panels that are brighter than  $V_0 = 14.0$ . At

<sup>5</sup> Updated version available online at <http://www.astro.utoronto.ca/~cclement/cat/listngc.html>

<sup>6</sup> Clement & Sawyer Hogg (1978) point out that the only Galactic GCs having more Type II Cepheids than M19 are  $\omega$  Cen and M14.

<sup>7</sup> Use of a color difference has the advantage of only a weak dependence on interstellar extinction; a formula for the extinction correction as a function of  $E(B - V)$  is given in Paper I.

<sup>3</sup> IRAF was distributed by the National Optical Astronomy Observatory, operated by the Association of Universities for Research in Astronomy (AURA) under a cooperative agreement with the National Science Foundation.

<sup>4</sup> <http://vizier.cfa.harvard.edu/viz-bin/VizieR-3?-source=I/345/gaia2>

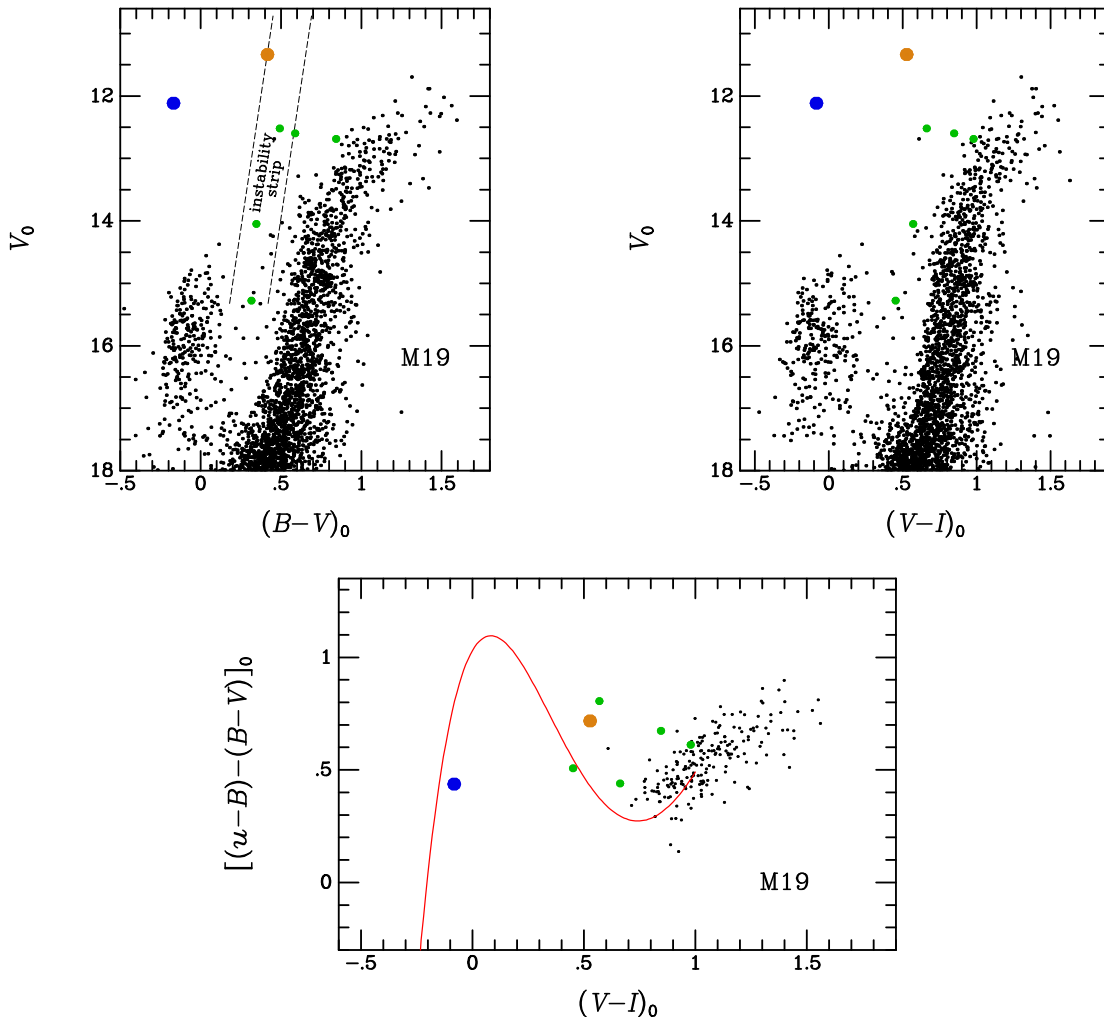


**Figure 1.** Top panels: Color-magnitude diagrams for M19 in  $V, B - V$  and  $V, V - I$ . Our photometry has been corrected for foreground reddening of  $E(B - V) = 0.38$ , and *Gaia* DR2 proper motions and parallaxes have been used to reject field stars (see text). The filled orange and blue circles show the locations of the two luminous PAGB stars belonging to the cluster. Dashed lines indicate the location of the pulsational instability strip. Filled green circles mark one RR Lyrae variable (the faintest object) and four Type II Cepheids. Bottom panel: Gravity-sensitive  $(u - B) - (B - V)$  color index, corrected for extinction and plotted against the temperature-sensitive  $V - I$  color, for stars brighter than  $V_0 = 14$  (black points). The red curve is a polynomial fit to the location of the HB in a sample of GCs with redder HBs than M19’s, taken from D21. The yellow PAGB star (filled orange circle), and the Cepheids, stand out from the HB locus because of their lower gravities and larger Balmer jumps. The blue PAGB star (filled blue circle) is hotter, and lies in the regime where the size of the Balmer jump depends on temperature rather than surface gravity.

these bright magnitudes, nearly all of the M19 stars are red giants or AGB stars. The selection criterion for yellow PAGB stars is that they have a Balmer-jump index significantly larger (i.e., redder) than do HB stars at the same color, and that they are at least 3 magnitudes brighter than the HB at the same color. As the top panels show, the HB in M19 is extremely blue, and almost entirely lacks stars on the cooler “horizontal” locus of the HB. Therefore, as an indicator of the HB’s location, we use a polynomial fit to the mean location of the HB in a sample of GCs with redder HBs, taken from D21. This relation is plotted as a red line in the bottom panel

of Figure 1. The peak in this sequence on the left-hand side of the diagram, at  $(V - I)_0 \simeq 0.1$ , is due to the maximum size of the Balmer jump at this color on the HB.

The single RR Lyrae star in M19 (included in the bottom panel of Figure 1 in spite of being fainter than  $V_0 = 14.0$ ) does lie almost exactly on the mean HB locus. The four Cepheids fall above the HB relation, consistent with their higher luminosities, lower surface gravities, and consequent higher  $(u - B) - (B - V)$  color differences. There also appears to be an above-the-HB (AHB) member of M19 at  $V_0 \simeq 12.7$  with a high value of

the color difference; curiously, although this star apparently lies within the instability strip, it is not a known variable. This object, and other AHB stars in Galactic GCs, will be discussed in D21.

The most conspicuous star in the three panels of Figure 1 is the very bright object plotted as an orange filled circle. It has a Balmer jump larger than those of HB stars, as shown in the bottom panel, making it a strong candidate for a yellow PAGB star.

Also conspicuous in the Figure 1 CMD is a bright, very blue star. For stars this hot, the  $(u - B) - (B - V)$  color difference is no longer sensitive to surface gravity (see Paper I, Figures 4 and 5), becoming instead a temperature index. This star is a candidate luminous blue PAGB star.

Both objects had been marked as candidate UV-bright stars in the classical ZNG study; our yellow PAGB star is M19 ZNG 4, and the blue one is M19 ZNG 2. To our knowledge, the present study is the first to present evidence that both of them are luminous members of the cluster, rather than foreground objects.

The left panel in Figure 2 presents a finding chart for the yellow and blue PAGB stars in M19, made from one of our  $B$ -band frames. To illustrate how conspicuous these two stars are in the ground-based UV, the right panel in Figure 2 shows a  $u$ -band frame. The two PAGB stars dominate this image. (The bright star to the NW of the blue PAGB star is the brightest Type II Cepheid in M19, V1, which was marked as the UV-bright object ZNG 3 in the ZNG study. The bright star to the NE of the blue PAGB star is ZNG 1, a foreground field object, as indicated by its *Gaia* parallax and proper motion. Two more UV-bright candidates, further from the cluster center, designated ZNG 5 and 6, are also non-members, according to *Gaia* astrometry.)

Table 1 presents basic data for our two PAGB candidates. The *Gaia* Early Data Release 3 (EDR3; [Gaia Collaboration et al. 2020](#)) became available as we were completing this paper, and is the source for the astrometry given in rows 1 through 5 of the table. The radial velocity (RV) for the yellow PAGB star in row 6 is from *Gaia* DR2. Rows 7 through 10 give our  $uBVI$  photometry. The interstellar reddenings in row 11 are taken from the high-resolution M19 extinction maps of [Alonso-García et al. \(2012\)](#) and [Johnson et al. \(2017\)](#). The former map is based on stellar photometry with the Magellan Telescope, and the latter on stellar photometry using *Hubble Space Telescope* (*HST*) images.<sup>8</sup>

The reddening values from these two maps agree well [the differences in  $E(B - V)$  at the locations of the two stars are 0.006 and 0.013 mag, respectively], and we give their means in Table 1. However, it should be noted that there are appreciable variations in  $E(B - V)$  from cell to cell in both extinction maps, and it is difficult to estimate the uncertainty in the reddening for an individual star. We adopt  $\pm 0.02$  mag as a reasonable guess.

#### 4. CLUSTER DISTANCE AND VISUAL ABSOLUTE MAGNITUDES

To convert the apparent magnitudes in row 7 of Table 1 to absolute magnitudes, we need the distance to the cluster. For M19, distance determinations from photometric methods are unusually problematic, for at least two reasons. First, the relatively large and spatially variable reddening makes the correction for extinction difficult. Second, distance methods based on the HB suffer because, in the case of M19 (as shown in Figure 1), the cluster’s “horizontal” branch is nearly vertical in CMDs made at optical wavelengths.

With the recent availability of *Gaia* EDR3, it is also possible to obtain a direct geometric distance estimate. We considered the sample of 202 RGB cluster members brighter than  $V_0 = 14$ , which we had chosen for the bottom panel in Figure 1. The mean EDR3 parallax for this sample, and its standard error, are  $0.0934 \pm 0.0062$  mas. To this we applied the global zero-point offset of  $+0.017$  mas from the analysis of [Lindegren et al. \(2020\)](#).

In Table 2 we list six distance determinations, made using a variety of essentially independent techniques, as summarized in the notes to the table. We see no compelling reason to adopt one of these determinations, so we will use a weighted mean of the four determinations for which uncertainties are given (and which, as it happens, span the range of distances found by these studies). This results in our adopted distance modulus of  $(m - M)_0 = 14.84 \pm 0.06$  ( $d = 9.29 \pm 0.26$  kpc).

Row 12 in Table 1 gives the visual absolute magnitudes of both stars, calculated from our photometry, the interstellar extinction given in row 11 (using  $R_V = 3.1$ ), and the distance modulus adopted in this section. The stated formal uncertainties are likely somewhat optimistic, given the possibilities of systematic errors in the extinction and distance.

sent us a numerical table giving the extinction map depicted in Figure 2 of [Johnson et al. \(2017\)](#). Unfortunately the existing *HST* frames cannot be used for optical photometry of the bright PAGB stars because their images are saturated.

<sup>8</sup> The Alonso-García et al. reddening map is presented pictorially in their Figure 13, and in tabular form at <https://vizier.u-strasbg.fr/viz-bin/VizieR-4>. C. Johnson kindly

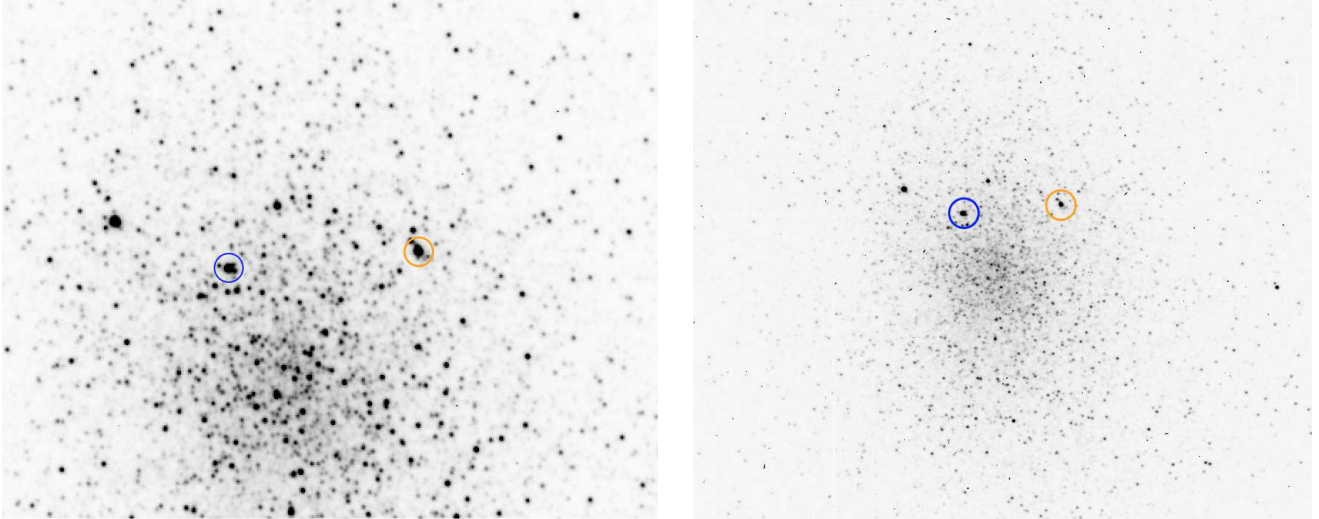


**Figure 2.** Left panel: finding chart for the yellow PAGB star (orange circle) and the blue PAGB star (blue circle) in the globular cluster M19. Made from a  $B$ -band CCD frame obtained with the CTIO 0.9-m telescope. North is at the top, east on the left; frame is  $2'5$  high. Right panel:  $u$ -band frame from same telescope, height  $4'8$ , illustrating how conspicuous both stars are in the ground-based ultraviolet. (The bright star to the NE of the blue PAGB star is a foreground object, ZNG 1. The bright star to the NW is the Type II Cepheid V1 = ZNG 3.)

**Table 1.** Basic Data for the Luminous Post-AGB Stars in M19

Parameter	“Yellow” PAGB (M19 ZNG 4)	“Blue” PAGB (M19 ZNG 2)	Source <sup>a</sup>
R.A. [J2000]	17:02:35.186	17:02:39.155	(1)
Dec. [J2000]	−26:15:24.14	−26:15:29.36	(1)
Parallax [mas]	$+0.119 \pm 0.016$	$+0.158 \pm 0.024$	(1)
R.A. proper motion [mas yr <sup>−1</sup> ]	$−2.878 \pm 0.019$	$−2.990 \pm 0.025$	(1)
Dec. proper motion [mas yr <sup>−1</sup> ]	$+1.146 \pm 0.012$	$+1.454 \pm 0.018$	(1)
Radial velocity [km s <sup>−1</sup> ]	$+142.3 \pm 1.4$	...	(2)
$V$	$12.512 \pm 0.006$	$13.291 \pm 0.006$	(3)
$u - B$	$1.471 \pm 0.012$	$0.608 \pm 0.015$	(3)
$B - V$	$0.795 \pm 0.010$	$0.211 \pm 0.010$	(3)
$V - I$	$1.021 \pm 0.011$	$0.390 \pm 0.010$	(3)
Reddening, $E(B - V)$	$0.344 \pm 0.020$	$0.342 \pm 0.020$	(4)
Absolute magnitude, $M_V$	$−3.39 \pm 0.09$	$−2.61 \pm 0.09$	(5)
Absolute luminosity, $\log L/L_\odot$	3.24	3.22	(6)

<sup>a</sup>Sources: (1) *Gaia* EDR3; (2) *Gaia* DR2; (3) This paper (not corrected for extinction); note that the zero-point for the  $u$  magnitude is such that  $u = 1.0$  for Vega; (4) From the reddening maps of [Alonso-García et al. \(2012\)](#) and [Johnson et al. \(2017\)](#) (see the text, §3); (5) This paper, calculated from data in this table,  $R_V = 3.1$ , and a distance modulus of  $(m - M)_0 = 14.84 \pm 0.06$  mag (see the text, §4); (6) This paper, calculated from data in this table, and bolometric corrections from [Castelli & Kurucz \(2004\)](#) (see the text, §7).

## 5. CLUSTER-MEMBERSHIP TESTS

Both of the PAGB candidates lie well within the spatial boundaries of the cluster (see Figure 2): the yellow and blue stars fall  $50''$  and  $36''$  from the cluster cen-

ter, respectively, which are within the half-light radius of  $79''2$ . Moreover, they have  $uBVI$  colors that are extremely unusual for field stars. Thus it is already highly probable that they are members of the cluster.

**Table 2.** M19 Distance Determinations

Distance [kpc]	$(m - M)_0$	Source
$8.99 \pm 0.83$	$14.77 \pm 0.20$	Piotto et al. (1999) <sup>a</sup>
$9.95 \pm 0.37$	$14.99 \pm 0.08$	Recio-Blanco et al. (2005) <sup>b</sup>
8.24	14.58	Valenti et al. (2007) <sup>c</sup>
8.79	14.72	Harris (2010) <sup>d</sup>
$8.13 \pm 0.47$	$14.55 \pm 0.13$	Baumgardt et al. (2019) <sup>e</sup>
$9.06 \pm 0.51$	$14.78 \pm 0.12$	This paper, <i>Gaia</i> EDR3 <sup>f</sup>

<sup>a</sup>Distance determined from luminosity of red-giant bump in *HST*-based *BV* color-magnitude diagram.

<sup>b</sup>Distance calculated by us by subtracting  $3.1E(B - V)$  from the value of  $(m - M)_{F555W} = 16.04 \pm 0.08$ , and adopting  $E(B - V) = 0.34$ , as given by Recio-Blanco et al. (2005).

<sup>c</sup>Distance determined from near-IR photometry of stars on the red-giant branch. Uncertainty not given.

<sup>d</sup>Distance calculated by us by subtracting  $3.1E(B - V)$  from the value of  $(m - M)_V = 15.90$ , and adopting  $E(B - V) = 0.38$ , as given by Harris (2010). Uncertainty not given.

<sup>e</sup>“Kinematic” distance derived from cluster-member proper-motion and radial-velocity dispersions and *N*-body modeling.

<sup>f</sup>Calculated by us based on the mean *Gaia* EDR3 parallax of a sample of cluster red giants, as described in §4.

Two further membership tests are possible: (1) RV, and (2) proper motion. Parallax is a less useful criterion for individual stars at the large adopted distance of M19, which corresponds to a parallax of only 0.108 mas. Nevertheless, the *Gaia* EDR3 parallaxes for both stars, given in row 3 of Table 1, corrected for the +0.017 zero-point offset (Lindegren et al. 2020), agree with the nominal value to within  $1.8$  and  $2.8\sigma$ , respectively.

*Gaia* EDR3 did not give RVs for either star, but the earlier DR2 listed a RV of  $+142.3 \pm 1.4 \text{ km s}^{-1}$  for the yellow PAGB star. This agrees extremely well with the mean cluster RV of  $+145.54 \pm 0.59 \text{ km s}^{-1}$  (Baumgardt et al. 2019); the velocity dispersion in the cluster is  $11.0 \text{ km s}^{-1}$  (Baumgardt & Hilker 2018). *Gaia* DR2 and EDR3 did not list a RV for the early-type blue PAGB candidate.

To make proper-motion membership tests for the two stars, we selected nearly pure samples of M19 members from *Gaia* EDR3. We chose stars lying within  $30''$  of each object, brighter than magnitude  $G = 18$ , redder than  $BP - RP = 1.2$ , and having a parallax less than 1 mas. The proper motions for these samples are plotted as black points in the two panels in Figure 3, with the proper motions of the PAGB candidates themselves

(rows 4 and 5 in Table 1) marked with orange and blue open circles. The *Gaia* CMDs of these two samples indicate that a large majority of the stars are cluster members lying on the RGB. In both cases, the motions of the PAGB candidates are well within the distributions of the cluster members. To illustrate the proper-motion distribution in the surrounding field, we selected stars from EDR3 in a nearby field, with a radius of  $200''$  and the same criteria. These are plotted as red points in the two figures; they show a wide range of proper motions, most of them in fact outside the range plotted.

In summary, the available evidence strongly confirms that both stars are physical members of M19.

## 6. VARIABILITY

As shown in the top left panel in Figure 1, the M19 yellow PAGB star lies close to the instability strip in the CMD. Several field analogs of the yellow PAGB stars in GCs are known to be low-amplitude semi-regular variables, including HD 46703 and BD+14°3061. As discussed in B20 (and references therein), both field stars have typical pulsation periods of  $\sim 29$ – $32$  days, and peak-to-peak amplitudes of  $\sim 0.1$ – $0.3$  mag. The pulsation amplitudes are variable; in the case of BD+14°3061, the variations can actually drop below detectability for extended intervals.

The most recent extensive search for variable stars in M19 of which we are aware is the photographic study by Clement & Sawyer Hogg (1978); this investigation did not mark the yellow PAGB star as variable. Our own *uBVI* data are of limited value, since we only have the two epochs in 1998 April separated by one day, plus an earlier lower-quality CCD observation obtained with the CTIO 1.5-m in 1995, which we did not include in our calibrated photometric reductions. We see no convincing evidence for variability in this limited material at a level of more than a few hundredths of a magnitude. The available data from current all-sky monitoring programs with small telescopes are generally of limited use, because of the crowding within the cluster. The uncertainty given for the *G* magnitude in *Gaia* EDR3 is very small, consistent with little or no variability.

Thus there is no evidence that the yellow PAGB star is variable, but additional monitoring observations with sufficient spatial resolution would be useful. (There is also no evidence that the blue PAGB star is variable, based on the same material.)

## 7. SPECTRAL-ENERGY DISTRIBUTIONS

We determined SEDs for both PAGB stars by combining our optical photometry from Table 1 with public data from the following sources:

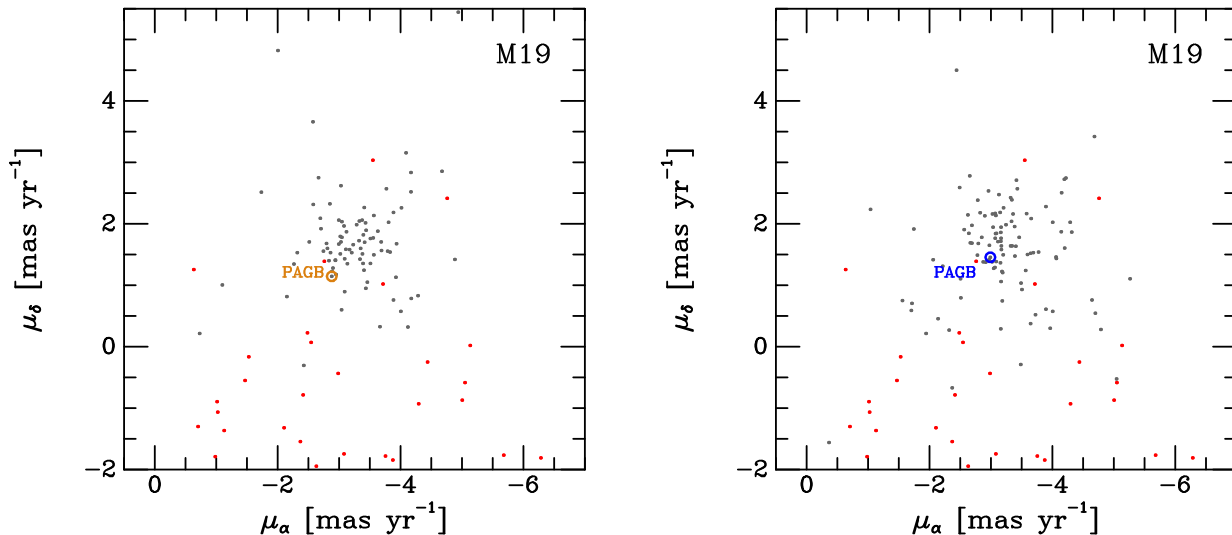


**Figure 3.** Left panel: Proper motions from *Gaia* EDR3 for stars within  $30''$  of the yellow P AGB star in M19, with parallax less than 1 mas, brighter than  $G = 18$ , and  $BP - RP$  color redder than 1.2 (black points). The color-magnitude diagram of these stars (not shown) indicates that nearly all of them are cluster members on the red-giant branch. The proper motion of the yellow P AGB star is marked with an orange circle. Right panel: Proper motions from EDR3 for stars within  $30''$  of the blue P AGB star in M19, selected with the same criteria (black points). The proper motion of the blue P AGB star is marked with a blue circle. In both panels the red points show the proper motions of stars in a nearby field, selected using the same criteria. The proper motions of both stars are well within the distributions of cluster members.

(1) The *Galaxy Evolution Explorer* (*GALEX*) (Morrissey et al. 2007) imaged M19 in its all-sky UV survey,<sup>9</sup> but only in its far-UV (FUV) bandpass. Although our blue P AGB star is prominent at FUV wavelengths, it is not contained in the *GALEX* source catalog (presumably because of crowding near the cluster center). We obtained the FUV image and, because the blue P AGB is so much brighter than its neighboring objects at FUV wavelengths, we measured its brightness using simple aperture photometry. We then translated these raw magnitudes into the standard flux system by scaling our measurements to similar aperture photometry of nearby isolated field stars with magnitudes given in the *GALEX* source catalog. The yellow P AGB star was too faint and blended to be measured in the FUV.

(2) The *Hubble Space Telescope* (*HST*) has imaged M19 on a few occasions,<sup>10</sup> but in nearly all of the frames the images of both P AGB stars are heavily saturated. We found an exposure of the blue P AGB star obtained with the Wide Field Planetary Camera 2 (WFPC2) in the near-UV (NUV) F255W filter (program GO-8718; PI G. Piotto), in which only the central pixel was saturated; we performed aperture photometry to obtain a lower limit on the star’s flux. For the yellow P AGB star, there are 10 WFPC2 frames in F255W (GO-10815; PI

Brown) with unsaturated images, on which we also performed aperture photometry. We used the PHOTFLAM keyword in the image headers to convert the counts to absolute fluxes, and applied the standard 0.10 mag correction to an infinite aperture. The *HST* images are virtually unaffected by source crowding.

(3) The UV/Optical Telescope (UVOT) on the Neil Gehrels *Swift* Observatory obtained images<sup>11</sup> of M19 in 2009 and 2010 in its three NUV/FUV bandpasses, *uvw1*, *uvw2*, and *uvw3*. We combined these images, and then performed PSF-fitting photometry of both P AGB stars using DAOPHOT. Corrections for time-dependent sensitivity loss, coincidence losses, and exposure time were applied, as detailed in Siegel et al. (2014); the data were then calibrated to the absolute photometric system of Breeveld et al. (2011). The *uvw1* and *uvw2* filters have substantial red leaks, which are problematic for cool stars; because of this, exacerbated by the considerable interstellar reddening, we did not include the observations of the yellow P AGB star in these two bandpasses in our analysis.

(4) The 2MASS near-infrared (NIR) sky survey (Skrutskie et al. 2006) obtained images of M19 in  $J$ ,  $H$ , and  $K_s$ . Photometry of our P AGB stars is contained in the 2MASS source catalog,<sup>12</sup> but is clearly affected by

<sup>9</sup> <https://galex.stsci.edu/GalexView/>

<sup>10</sup> <https://archive.stsci.edu/>

<sup>11</sup> <https://archive.stsci.edu/swiftuvot/>

<sup>12</sup> <https://irsa.ipac.caltech.edu/cgi-bin/Gator/nph-dd>

the stellar crowding near the cluster center. We therefore downloaded the 2MASS frames, and performed DAOPHOT PSF photometry on the images, calibrating to the 2MASS photometric zero-point using measurements of nearby isolated stars contained in the source catalog. *HST* images in the *I* (F814W) band show that the yellow PAGB star, at the 2MASS resolution, is blended with four nearby red giants. We attempted to de-blend the images, using the *HST* frame as a prior to define the precise locations of the PAGB stars in the 2MASS frames, but with limited success.

(5) Images of M19 were obtained in 2013 with the warm *Spitzer Space Telescope* and its Infrared Array Camera (IRAC), in the 3.6 and 4.5  $\mu\text{m}$  bandpasses; the observations were part of a program aimed at RR Lyrae stars (PI W. Freedman). We downloaded a selection of these images<sup>13</sup> and performed DAOPHOT photometry to de-blend the stellar images, using PSF fitting radii of the order of the FWHM. Aperture corrections were then applied, based on the total magnitudes of isolated field stars in the frames.

(6) We examined NIR and far-IR images of M19 from the *Wide-Field Infrared Survey Explorer (WISE)* sky survey, which we downloaded from SkyView.<sup>14</sup> However, the spatial resolution of these frames is far too poor to provide useful photometry for our targets lying in very crowded regions of the cluster.

We then corrected all of the measured fluxes for interstellar extinction, using the values of  $E(B - V)$  in Table 1, and for most bandpasses applying the formulae of Cardelli et al. (1989), calculated at the effective wavelength of each bandpass, and assuming  $R_V = 3.1$ . For the UVOT photometry, because of the complex structure of the extinction curve around 2200  $\text{\AA}$ , we determined the extinction corrections by integrating the Cardelli et al. formula convolved with the system throughput curves and a blackbody function having the approximate temperature of each star. For the two IRAC bandpasses, whose wavelengths are beyond the range of the Cardelli et al. formulae, we determined the extinction at the  $K_s$  band, and scaled it to [3.6] and [4.5] according to the relations given by Indebetouw et al. (2005). The resulting extinction-corrected fluxes must be regarded as only approximate, given the very large correction factors in the UV, the uncertainty whether  $R_V = 3.1$  is appropriate for this line of sight, and the source crowding in many of the bandpasses.

The two panels in Figure 4 plot the SEDs for the two PAGB stars. We superpose model-atmosphere SEDs selected from the ATLAS9 grid<sup>15</sup> of Castelli & Kurucz (2004). The metal abundances for these SEDs are  $[M/H] = -1.5$ , with  $\alpha$ -element enhancements. We adopted surface gravities of  $\log g = 0.5$  and 2.0 for the yellow and blue PAGB stars, respectively. The best fits to the SEDs are found for effective temperatures of 6250 and 11750 K, respectively, but we caution that there is some degeneracy between the adopted  $T_{\text{eff}}$  values and reddenings.

Using the bolometric corrections for the two Castelli & Kurucz models, we find the absolute luminosities given in the final row of Table 1,  $\log L/L_\odot = 3.24$  and 3.22 for the yellow and blue PAGB stars, respectively. Thus their luminosities are nearly identical, and they are likely to be on very similar post-AGB evolutionary tracks.

A primary aim in investigating the SEDs was to search for evidence of circumstellar dust, ejected during the AGB phase. In general, circumstellar dust has not been found to be prominent in yellow and blue PAGB stars in old populations, such as those in GCs (e.g., B16 and B20), possibly because the PAGB evolutionary timescales are slow enough for any ejecta to have dissipated, combined with the difficulty of forming dust in a low-metallicity environment. As Figure 4 shows, we likewise see no evidence for warm circumstellar dust in the two M19 PAGB stars. Unfortunately, the available observations only go out to the *Spitzer* [4.5] bandpass; the stellar crowding in the cluster precludes photometry at longer wavelengths with instruments such as *WISE*. Thus the constraints on dust are not very tight.

## 8. DISCUSSION AND FUTURE STUDIES

### 8.1. Yellow PAGB Stars as Standard Candles

The main goal of our *uBVI* survey was to search the Galactic GC system for yellow PAGB stars and to test them as potential Population II standard candles. The yellow PAGB star in M19 reported in this paper joins the small number of known objects of this class. We find it to have a visual absolute magnitude of  $M_V = -3.39 \pm 0.09$ , based on several recent determinations of the distance to M19. The main contributors to the error are the uncertainties in the cluster's distance, and in the foreground extinction.

B16 listed (their Table 4) the visual absolute magnitudes of the four other known non-variable yellow PAGB stars in Galactic GCs; they range from  $M_V = -3.10$  to  $-3.46$ . Adding our new result for the M19 star, and

<sup>13</sup> <https://sha.ipac.caltech.edu/applications/Spitzer/SHA/>

<sup>14</sup> <https://skyview.gsfc.nasa.gov/current/cgi/query.pl>

<sup>15</sup> <http://wwwuser.oats.inaf.it/castelli/grids.html>

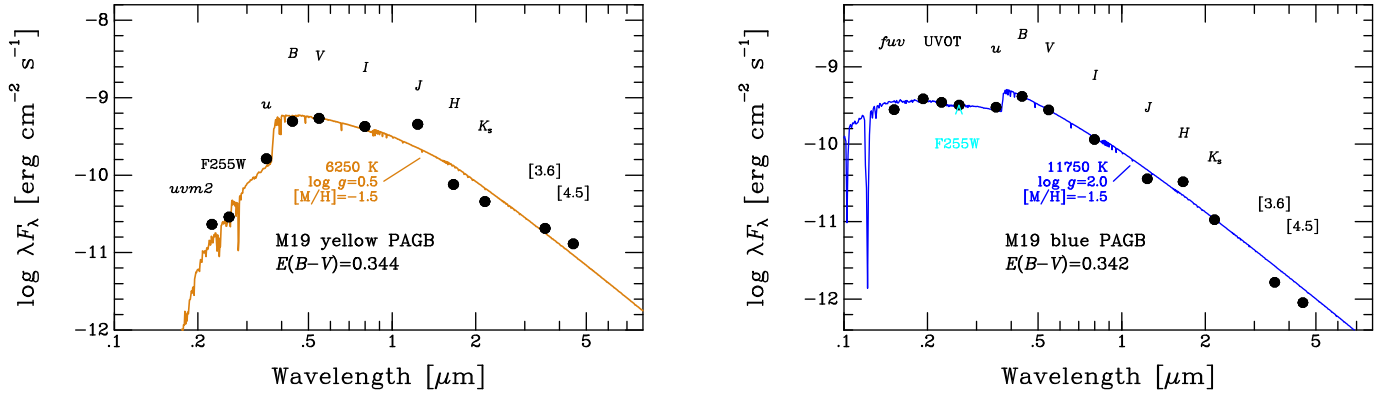


**Figure 4.** Left panel: Spectral-energy distribution for the M19 yellow PAGB star (filled black circles), corrected for interstellar reddening of  $E(B - V) = 0.344$  as described in the text. The orange curve is a model-atmosphere SED for a star with the parameters indicated in the figure. Note the conspicuously large Balmer discontinuity. Right panel: SED for the M19 blue PAGB star (filled black circles), corrected for  $E(B - V) = 0.342$ . The *HST* observation at F255W (cyan plotting point and label) is a lower limit (see text). The blue curve is a model-atmosphere SED with parameters indicated in the figure. See the text for details of the various public sky surveys used to assemble these SEDs, and caveats about uncertainties due to blending and the extinction corrections.

including also the absolute magnitude for the field yellow PAGB star BD+14°3061 from B20, we find that these six objects have a mean absolute magnitude of  $M_V = -3.35 \pm 0.06$ , with a standard deviation of 0.14 mag. This is a very narrow luminosity function, compared for example to that of Population I Cepheids at a given pulsation period (e.g., Clementini et al. 2019). And the discovery and measurement of yellow PAGB stars requires only a single observation epoch. Thus, we believe that these stars continue to be potential extragalactic distance indicators.<sup>16</sup> In several forthcoming papers, we will further explore this possibility.

We also note that the five yellow PAGB stars in Galactic GCs all belong to clusters with “intermediate” metallicities, of  $[\text{Fe}/\text{H}] = -1.59$  (NGC 5986),  $-1.60$  (M79),  $-1.74$  (M19), and  $-1.53$  ( $\omega$  Cen), as tabulated by H10. (However, M19 [see §2] and  $\omega$  Cen have fairly wide ranges of  $[\text{Fe}/\text{H}]$  among their members.) Moreover, all four clusters contain very blue HB stars. We will discuss these and other clues to the evolutionary status of these stars in more detail in papers now in preparation.

## 8.2. Future Work

There are several desirable future investigations of these two new and relatively bright PAGB stars in M19. First, moderate-resolution spectra should be obtained in order to confirm even more definitively that both stars are indeed low-metallicity cluster members, consistent

with the interpretations in this paper. High-resolution spectroscopic abundance studies of both of them would be of considerable interest, given the peculiarities seen in other PAGB stars. For example, Şahin & Lambert (2009) found an anomalously low iron abundance in the yellow PAGB star in M79, and several PAGB stars in younger populations show extreme depletions of refractory chemical elements with high condensation temperatures (see Oomen et al. 2019 and references therein). Several field PAGB stars appear to be long-period spectroscopic binaries (B20 and references therein), so RV monitoring would be useful to investigate whether binary interactions play a role in the evolution of these objects. Effective temperatures of the stars determined from model-atmosphere fitting, compared to the observed colors, would help refine the estimates of reddening, and thus of their absolute magnitudes. High-precision photometric monitoring would be useful to test whether the yellow PAGB star is a low-amplitude pulsating variable. High-spatial-resolution MIR photometry would provide tighter limits on circumstellar dust than was possible in the study reported here.

The observational work in 1998 was partially supported by NASA grant NAG 5-6821 under the “UV, Visible, and Gravitational Astrophysics Research and Analysis” program, and by the Director’s Discretionary Research Fund at STScI. H.E.B. thanks the staff at Cerro Tololo for their support over the years.

This work has made use of data from the European Space Agency (ESA) mission *Gaia* (<https://www.cosmos.esa.int/gaia>) processed by the *Gaia* Data Processing and Analysis Consortium (DPAC, <https://www.cosmos.esa.int/web/gaia/dpac/>). Funding for the DPAC has been provided by national

<sup>16</sup> If we had used its yellow PAGB star to estimate the distance to M19, using the zero-point of  $M_V = -3.38 \pm 0.05$  found earlier by B16, we would have obtained  $(m - M)_0 = 14.83 \pm 0.08$ . This agrees extremely well with the mean distance modulus from several independent methods of  $(m - M)_0 = 14.84 \pm 0.06$ , which we discussed in §4.

institutions, in particular the institutions participating in the *Gaia* Multilateral Agreement.

Based in part on observations made with the NASA Galaxy Evolution Explorer. *GALEX* was operated for NASA by the California Institute of Technology under NASA contract NAS 5-98034.

Based in part on observations made with the NASA/ESA *Hubble Space Telescope*, obtained from the data archive at the Space Telescope Science Institute. STScI is operated by the Association of Universities for Research in Astronomy, Inc. under NASA contract NAS 5-26555.

We acknowledge the use of public data from the Neil Gehrels *Swift* Observatory data archive.

This publication makes use of data products from the Two Micron All Sky Survey, which is a joint project

of the University of Massachusetts and the Infrared Processing and Analysis Center/California Institute of Technology, funded by the National Aeronautics and Space Administration and the National Science Foundation.

This work is based in part on observations made with the *Spitzer Space Telescope*, operated by the Jet Propulsion Laboratory, California Institute of Technology under a contract with NASA.

It also makes use of data products from the *Wide-field Infrared Survey Explorer*, which is a joint project of the University of California, Los Angeles, and the Jet Propulsion Laboratory/California Institute of Technology, funded by the National Aeronautics and Space Administration.

*Facilities:* CTIO 0.9m, Gaia, GALEX, 2MASS, Swift, HST, Spitzer, WISE

## REFERENCES

- Alonso-García, J., Mateo, M., Sen, B., et al. 2012, *AJ*, 143, 70
- Alves, D. R., Bond, H. E., & Onken, C. 2001, *AJ*, 121, 318
- Baumgardt, H. & Hilker, M. 2018, *MNRAS*, 478, 1520
- Baumgardt, H., Hilker, M., Sollima, A., et al. 2019, *MNRAS*, 482, 5138
- Bond, H. E. 1977, *BAAS*, 9, 601
- Bond, H. E. 1997a, in *IAU Symp. 180, Planetary Nebulae*, ed. H. J. Habing & H. J. G. L. M. Lamers (Dordrecht: Kluwer), 460
- Bond, H. E. 1997b, in *The Extragalactic Distance Scale*, ed. M. Livio, M. Donahue, & N. Panagia (Cambridge: Cambridge Univ. Press), 224
- Bond, H. E. 2005, *AJ*, 129, 2914 (Paper I)
- Bond, H. E. 2020, *AJ*, 160, 274 (B20)
- Bond, H. E., Ciardullo, R., & Siegel, M. H. 2016, *AJ*, 151, 40 (B16)
- Breeveld, A. A., Landsman, W., Holland, S. T., et al. 2011, in *AIP Conf. Proc. 1358, Gamma Ray Bursts*, ed. J. E. McEnery, J. L. Racusin, & N. Gehrels (Melville, NY: AIP), 373
- Cardelli, J. A., Clayton, G. C., & Mathis, J. S. 1989, *ApJ*, 345, 245
- Castelli, F., & Kurucz, R. L. 2004, arXiv:astro-ph/0405087
- Clement, C. M., Muzzin, A., Dufton, Q., et al. 2001, *AJ*, 122, 2587
- Clement, C. C., & Sawyer Hogg, H. 1978, *AJ*, 83, 167
- Clementini, G., Ripepi, V., Molinaro, R., et al. 2019, *A&A*, 622, A60
- Davis, B. D., Bond, H. E., Siegel, M. H., & Ciardullo, R. 2021, in preparation (D21)
- Dean, J. F., Warren, P. R., & Cousins, A. W. J. 1978, *MNRAS*, 183, 569
- Gaia Collaboration, Brown, A. G. A., Vallenari, A., et al. 2018, *A&A*, 616, A1
- Gaia Collaboration, Brown, A. G. A., Vallenari, A., et al. 2020, arXiv:2012.01533
- Gaia Collaboration, Helmi, A., van Leeuwen, F., et al. 2018, *A&A*, 616, A12
- Gaia Collaboration, Prusti, T., de Bruijne, J. H. J., et al. 2016, *A&A*, 595, A1
- Gonzalez, G., & Wallerstein, G. 1992, *MNRAS*, 254, 343
- Harris, W. E. 2010, arXiv:1012.3224 (H10)
- Harris, H. C., Nemec, J. M., & Hesser, J. E. 1983, *PASP*, 95, 256
- Harris, W. E., Racine, R., & de Roux, J. 1976, *ApJS*, 31, 13
- Indebetouw, R., Mathis, J. S., Babler, B. L., et al. 2005, *ApJ*, 619, 931
- Johnson, C. I., Caldwell, N., Rich, R. M., et al. 2017, *ApJ*, 836, 168
- Jones, D. H. P. 1968, *MNRAS*, 140, 265
- Kruijssen, J. M. D., Pfeffer, J. L., Chevance, M., et al. 2020, *MNRAS*, 498, 2472
- Landolt, A. U. 1992, *AJ*, 104, 340
- Lindgren, L., Bastian, U., Biermann, M., et al. 2020, arXiv:2012.01742
- Moehler, S., Landsman, W. B., Lanz, T., et al. 2019, *A&A*, 627, A34

- Morrissey, P., Conrow, T., Barlow, T. A., et al. 2007, *ApJS*, 173, 682
- Oomen, G.-M., Van Winckel, H., Pols, O., et al. 2019, *A&A*, 629, A49
- Pfeffer, J., Lardo, C., Bastian, N., et al. 2020, *MNRAS*, in press
- Piotto, G., Zoccali, M., King, I. R., et al. 1999, *AJ*, 118, 1727
- Recio-Blanco, A., Piotto, G., de Angeli, F., et al. 2005, *A&A*, 432, 851
- Şahin, T., & Lambert, D. L. 2009, *MNRAS*, 398, 1730
- Siegel, M. H. & Bond, H. E. 2005, *AJ*, 129, 2924 (Paper II)
- Siegel, M. H., Porterfield, B. L., Linevsky, J. S., et al. 2014, *AJ*, 148, 131
- Skrutskie, M. F., Cutri, R. M., Stiening, R., et al. 2006, *AJ*, 131, 1163
- Stetson, P. B. 1987, *PASP*, 99, 191
- Thuan, T. X., & Gunn, J. E. 1976, *PASP*, 88, 543
- Valenti, E., Ferraro, F. R., & Origlia, L. 2007, *AJ*, 133, 1287
- Zinn, R. J., Newell, E. B., & Gibson, J. B. 1972, *A&A*, 18, 390 (ZNG)